Anchored Metal-to-Metal Charge-Transfer Chromophores in a Mesoporous Silicate Sieve for Visible-Light Activation of Titanium Centers

Wenyong Lin and Heinz Frei*

Physical Biosciences Division, Mailstop Calvin Laboratory, Lawrence Berkeley National Laboratory, University of California, Berkeley, California 94720

Received: October 22, 2004

Binuclear metal-to-metal charge-transfer (MMCT) moieties consisting of a Ti and a Cu^{I} or a Ti and a Sn^{II} center were obtained in a MCM-41 silicate sieve along with isolated metal centers when exposing Ti-grafted MCM-41 to Cu^{I} or Sn^{II} precursors featuring highly labile CH_3CN ligands. Fourier transform infrared (FT-IR) spectroscopy revealed complete removal of the labile CH_3CN ligands of the metal precursor and the formation of $Cu^{I}-O-Ti$, $Cu^{I}-O-Si$, and corresponding Sn^{II} linkages on the pore surface. Optical and FT-IR difference spectroscopy upon oxidation of Cu^{I} (Sn^{II}) allowed assignment of the $Cu^{I}-O$ (642 cm^{-1}) and $Sn^{II}-O$ (610 cm^{-1}) bond modes of the MMCT moiety. The visible-light-absorbing $Ti^{IV}-O-Cu^{I}$ MMCT chromophore extends from the UV to 600 nm, the corresponding $Ti^{IV}-O-Sn^{II}$ absorption to 470 nm. Electron paramagnetic resonance monitoring of the $TiSn^{II}-$MCM-41 sieve following photoexcitation of the MMCT transitions at cryogenic temperature confirmed that Ti is reduced to Ti^{III} under visible light. Assembly of inorganic MMCT sites inside high-surface-area mesoporous silicates with each metal in a preselected oxidation state opens up activation of catalytically important metal centers under visible light.

1. Introduction

Transition metals that are part of the framework of micro- or mesoporous sieves or covalently attached to the pore walls of these materials function as active sites of interesting photocatalytic or photosynthetic transformations of adsorbed molecules. Most transition metal-mediated photoreactions in such porous inorganic frameworks, typically silicates or aluminophosphates, involve ligand-to-metal charge-transfer (LMCT) from framework oxygen to the metal center, resulting in a transiently reduced metal and a hole on a lattice oxygen.[1−4] However, LMCT transitions with oxygen as a donor typically lie in the UV region and are therefore inaccessible to solar photons. Moreover, use of UV light often leads to unselective chemistry due to secondary photolysis of primary products. A crucial challenge is therefore to find porous materials that afford redox chemistry of adsorbed molecules under visible light.

Photoactivation of framework or grafted transition metals in a molecular sieve could in principle be achieved with visible light if oxygen were replaced by a ligand with lower optical electronegativity, such as sulfur. However, oxygen ligands of transition metals tend to be substantially more stable, making the design of robust photoreactors based on ligands such as sulfur extremely challenging. However, engaging a second metal center as a donor linked to the first metal by an oxo bridge may offer a robust chromophore. Oxo-bridged metal-to-metal charge-transfer (MMCT) moieties of mixed metal oxides are known to absorb visible and even near-IR light.[5] The great flexibility in the selection of metal and oxidation state might open up access to solar-light-absorbing chromophores with a wide range of redox properties. Only a very few framework or anchored bimetallic moieties have been reported in mesoporous sieves,[6,7] and none have been explored thus far in terms of MMCT properties. While covalent anchoring of a variety of single metals on mesoporous silicate supports has been demonstrated, procedures typically require calcination for the removal of organic precursor ligands[8] that often results in a change of the nascent oxidation state. To allow free choice and control of the oxidation state of each metal, methods have to be developed that obviate the need for ligand removal by calcination.

We report in this paper $Ti^{IV}-O-Cu^{I}$ and $Ti^{IV}-O-Sn^{II}$ groups grafted onto a mesoporous MCM-41 silicate sieve. The goal is to establish the existence of the binuclear MMCT groups and demonstrate covalent anchoring by the direct observation of the metal−oxygen bonds on the pore surface. For exploration of MMCT absorptions, d^{10} or s^2 metals such as Cu^{I} or Sn^{II} offer a simple starting point because they lack ligand-field or low-energy ligand-to-metal charge-transfer bands that might complicate the spectra in the visible region. The bimetallic materials feature MMCT chromophores in a completely inorganic ligand environment that afford photoactivation of titanium centers under visible light. Photoreduction of Ti^{4+} to Ti^{3+} with long-wavelength photons is an important goal since it has been shown that activation of isolated titanium centers of framework-substituted silicates via LMCT excitation by UV light gives rise to interesting photocatalytic and photosynthetic transformations.[1−3]

2. Experimental Section

A MCM-41 sieve was prepared according to a method described previously.[9] Briefly, 2.2 g of cetyltrimethylammonium bromide (CTAB) template were dissolved in 52 mL of water at 40 °C. Ammonium hydroxide (Aldrich, 26 mL, 30%) was then added under stirring. Addition of 10 mL of tetraethoxysilane (Fluka, puriss.) to the solution was followed by continued stirring for 3 h at room temperature. The gel was transferred to a Teflon-lined autoclave and held at 110 °C for 48 h. Filtration

* Author to whom correspondence should be addressed. Phone: (510) 486-4325. Fax: (510) 486-6059. E-mail: Hmfrei@lbl.gov.

10.1021/jp040677z CCC: $30.25
Published on Web 02/24/2005

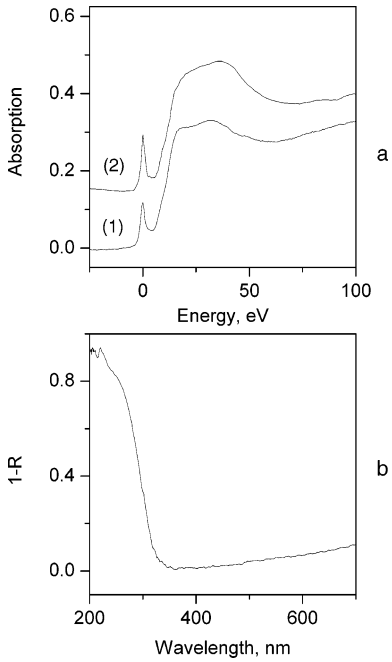

Figure 1. Spectroscopic characterization of grafted Ti−MCM-41. (a) Ti K-edge XANES spectra. The A_1-T_2 preedge peak position (4968 eV) is taken as the origin of the energy scale. Trace 1 shows the spectrum of a partially dehydrated wafer, trace 2 for the state of dehydration reached upon 24 h evacuation at room temperature. (b) UV−vis diffuse reflectance spectrum of calcined Ti−MCM-41 in a vacuum. R = reflectance; $BaSO_4$ is the reference.

and washing with distilled H_2O gave the product. Template removal was conducted by heating at 300 °C for 2 h followed by calcination in air at 550 °C for 12 h. Grafting of Ti onto MCM-41 was performed using the titanocene dichloride method by Maschmeyer et al.[8a] Reagents used were $TiCp_2Cl_2$ (Aldrich, 97%), triethylamine (Fluka, puriss.), and anhydrous chloroform (Aldrich, 99%). The synthesis was conducted in a dry nitrogen glovebox. The material was calcined at 550 °C for 5 h, resulting in organic-free Ti−MCM-41 with Si/Ti = 54 ± 2 according to inductively coupled plasma (ICP) analysis. X-ray absorption near-edge structure (XANES) spectra of the Ti K-edge of pressed wafers of Ti−MCM-41 recorded at the Advanced Light Source showed a sharp preedge peak at 4968 eV (for experimental details, see ref 10). The peak, shown in Figure 1a, is attributed to the A_1-T_2 absorption of tetrahedrally coordinated Ti centers. Its height relative to that of the K-edge (0.43−0.64 depending on the degree of dehydration, Figure 1a) is a measure of the fraction of Ti in tetrahedral coordination.[11] Comparison with literature XANES spectra of Ti−MCM-41 confirmed the high yield of tetrahedrally grafted Ti centers (0.5−0.6).[6b,12] Furthermore, the UV diffuse reflectance spectra of Ti−MCM-41 (Shimadzu model UV-2100 spectrometer equipped with integrating sphere model ISR-260) exhibit an absorption with an onset at 330 nm (Figure 1b). The sieve crystallites were pressed into a self-sustaining pellet and mounted in a home-built diffuse reflectance spectroscopy (DRS) vacuum cell.[13] The short-wavelength onset of the band shows that it is mainly due to the LMCT transition of tetrahedrally coordinated Ti, in agreement with literature spectra.[14]

A $TiCu^{I}$−MCM-41 sieve was synthesized by adding 0.2 g of freshly calcined Ti−MCM-41 powder to a 0.1 wt % solution of $Cu^{I}(NCCH_3)_4PF_6$ (Aldrich) in 100 mL of CH_2Cl_2 (Aldrich) in a N_2 glovebox. The crystallites turned instantly yellow, and the solution was stirred for 10 min at room temperature. The product was collected by filtration, washed 4 times with 50 mL aliquots of methylene chloride, and dried at room temperature. A typical Ti/Cu ratio was 0.82 ± 0.05 per ICP analysis. Note that the amount of grafted Cu is close to the Ti loading. For the preparation of monometallic Cu^{I}−MCM-41, the same grafting procedure was used with calcined MCM-41 as starting material. In this case, no coloration of the solution was noted. Assembly of $TiSn^{II}$ bimetallic chromophores in MCM-41 pores was conducted by adding 0.2 g of freshly calcined Ti−MCM-41 powder to a 0.1 wt % solution of $SnCl_2$ $2H_2O$ (Aldrich) in 100 mL of acetonitrile/dichloromethane 1:1 mixture. Stirring at room temperature for 10 min was followed by filtration, washing with dichloromethane, and drying at room temperature. All operations were performed in a N_2 glovebox. The hydrate was used because anhydrous $SnCl_2$ dissolved in acetonitrile only very slowly. Upon evacuation of the as-synthesized $TiSn^{II}$−MCM-41 at room temperature, Fourier transform infrared (FT-IR) spectroscopy confirmed complete removal of H_2O.[15] ICP analysis gave Ti/Sn = 1.92 ± 0.04. Powder X-ray diffraction (XRD) measurements (Siemens model D500 Cu Kα) of the bimetallic sieves showed no loss of long-range order upon grafting (Figure 2) as indicated by the observation of the same Bragg peaks as those reported for neat MCM-41.[16] No extra peak or phase was detected. High-surface-area TiO_2 powder (Alfa Aesar, 180−300 m^2g^{-1}) was subjected to heating at 500 °C for 4 h before use.

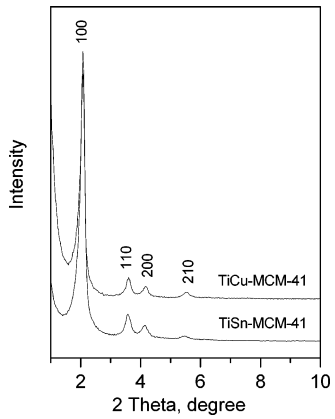

Figure 2. XRD patterns of as-prepared TiCu−MCM-41 and TiSn−MCM-41 measured in air. Hexagonal lattice indices are shown.[16]

For DRS measurements of $TiCu^{I}$−MCM-41, Cu^{I}−MCM-41, $TiSn^{II}$−MCM-41, or Sn^{II}−MCM-41, pressed wafers were loaded into the optical vacuum cell under an N_2 atmosphere. While mounted on the intergrating sphere, the cell was connected to a vacuum manifold for evacuation or loading of oxygen gas. The same procedure was used for loading of the sample into a transmission infrared vacuum cell equipped with CaF_2, KCl, or KBr windows.[17] FT-IR spectrometers used were Bruker model IFS88 or IFS66V equipped with liquid-nitrogen-cooled MCT detectors, Kolmar model KMPV8−1-J2 with an 8 μm band gap or Infrared Associates with a 25 μm band gap. As in the case of DRS experiments, the infrared cell was connected to a vacuum manifold equipped with a turbo-molecular pump (Varian Model V-70). DRS and FT-IR spectra of Cu^{I} or Sn^{II} grafted onto porous TiO_2 were recorded by using pressed wafers of a mixture with KBr. FT-Raman spectra were recorded with a Bruker model FRA-106/S module equipped with a Nd:YAG laser source and a liquid-nitrogen-cooled Ge detector.

Electron paramagnetic resonance (EPR) spectra were recorded at 20 K with a Varian spectrometer model E-109 featuring an E-102 microwave bridge. Crystallite powders were loaded into quartz EPR tubes in a N_2 glovebox, evacuated for 12 h at 200

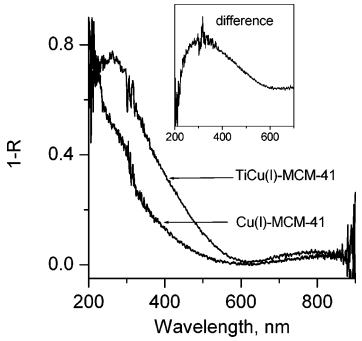

Figure 3. UV−vis DRS spectra of as-synthesized Cu^{I}−MCM-41 and $TiCu^{I}$−MCM-41 under vacuum. The insert shows the difference of $TiCu^{I}$ and Cu^{I} spectra.

°C and sealed under vacuum. Irradiation was conducted at 77 K by immersing the sealed EPR tubes into liquid N_2 inside a quartz dewar. For visible-light irradiation, the filtered emission of a W-source (Corning filter #3-75, $\lambda > 400$ nm, 2 W) was used. Excitation at 355 nm (160 mW cm^{-2}) was conducted with the third harmonic emission of a Quanta-Ray Nd:YAG laser model DCR-2A.

3. Results and Discussion

A. $TiCu^{I}$−MCM-41. The concept for assembling bimetallic sites on the mesopore surface is to have a Cu^{I} precursor react with the anchored titanol group[8a] of Ti−MCM-41. The choice of the Cu precursor complex was based on the need for very mild grafting conditions and for avoiding ligand removal by calcination. Weak acetonitrile complexes featuring noncoordinating, redox-stable anions such as PF_6^- in nonaqueous solvents are a source of bare metal ions.[18] Grafting is energetically driven by the formation of a Cu^{I}−O bond where before there was none (82 kcal mol^{-1}).[19] Furthermore, the TiOH group is more acidic than the SiOH group as manifested by the lower OH stretch frequency of TiOH (3676 cm^{-1})[2e,20a] compared to that of SiOH (3745 cm^{-1}).[20] Therefore, titanol groups are expected to be more reactive toward the Cu^{I} complex than silanol groups,[20f] resulting in a higher proportion of bimetallic sites relative to isolated centers than predicted by the relative abundance of TiOH and SiOH groups.

The diffuse reflectance spectrum of an evacuated sample (room temperature) of $TiCu^{I}$−MCM-41 exhibits an absorption tail extending from the UV to about 600 nm, as can be seen in Figure 3. This tail is not present in the spectrum of monometallic Cu^{I}−MCM-41, whose spectrum shows the $3d^{10} \rightarrow 3d^{9}4s^{1}$ UV absorption.[21] The difference of the two spectra, shown in the insert of Figure 3, is attributed to the $Ti^{IV}/Cu^{I} \rightarrow Ti^{III}/Cu^{II}$ MMCT transition.

Structural details of the grafted Cu^{I} and $TiCu^{I}$ moieties were revealed by in situ FT-IR spectroscopy. Evacuation of the as-synthesized material at room temperature results in grafted metal centers that still feature residual CH_3CN ligands. Trace a of Figure 4 shows the difference infrared spectra of Cu^{I}−MCM-41 and neat MCM-41. The bands in the ν(C−H) region (3007 and 2945 cm^{-1}), the ν(C≡N) region (2330 and 2302 cm^{-1}), and the CH bending region (1418 and 1375 cm^{-1}) are due to CH_3CN ligands attached to grafted Cu^{I} centers. No absorptions due to the $Cu^{I}(NCCH_3)_4PF_6$ precursor compound (2313, 2300, 2275, 842, 557 cm^{-1} (Nujol)) or physisorbed acetonitrile (3012, 2948, 2298, 2265, 1443, 1414, 1375, 922 cm^{-1} (MCM-41)) are observed.[15] Heating of the sample to 200 °C under vacuum led to complete desorption of residual CH_3CN ligands, as can be seen from trace b of Figure 4. Figure 5 shows the corresponding

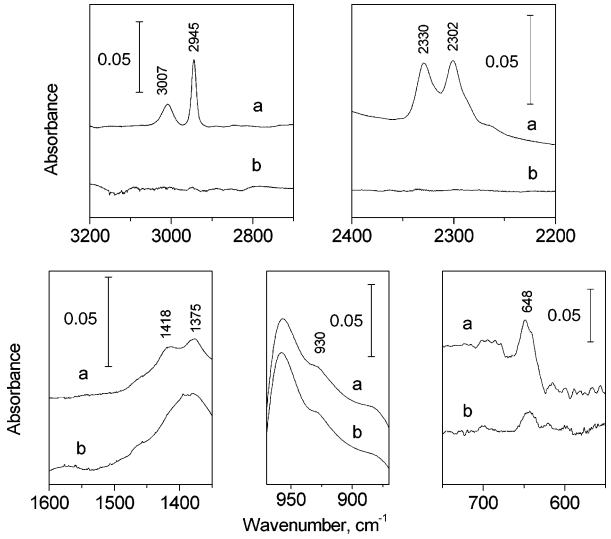

Figure 4. FT-IR spectra of Cu^{I}−MCM-41 wafers (a) as-synthesized, under vacuum and (b) after heating to 200 °C under vacuum. For background subtraction, the spectrum of neat MCM-41 was used. The very broad feature in the region 1500−1300 cm^{-1} is part of the background, caused by different infrared-light-scattering behavior of grafted and ungrafted MCM-41 silicate material. Spectra a and b were recorded for different samples.

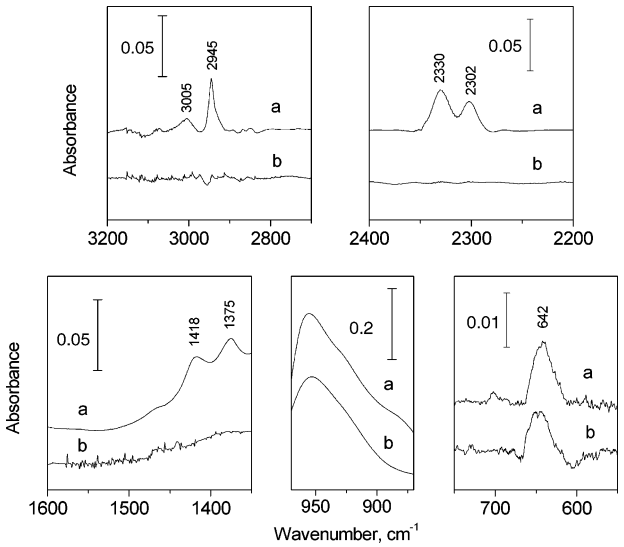

Figure 5. FT-IR spectra of $TiCu^{I}$−MCM-41 wafers (a) as-synthesized, under vacuum and (b) after heating to 200 °C under vacuum. For background subtraction, the spectrum of neat MCM-41 sieve was used. The baseline shift in the 1500−1300 cm^{-1} region is due to different light-scattering behavior of grafted and neat MCM-41 material.

infrared spectra upon grafting of the Cu^{I} complex onto Ti−MCM-41. Again, no absorptions due to $Cu^{I}(NCCH_3)_4^+$ were detected. Spectra of the bimetallic $TiCu^{I}$−MCM-41 sample before and after heating to 200 °C showed the same loss of residual CH_3CN ligands. The substantially larger amount of Cu^{I} grafted onto Ti−MCM-41 compared to that grafted onto MCM-41 evident from Figures 4 and 5 (see below) allowed the detection of a weak band at 836 cm^{-1} typical for the (intrinsically very intense) ν_3 mode of PF_6^-.[22] We attribute it to a small amount of anion adsorbed on the pores. The band was stable under heat treatment in a vacuum, indicating that PF_6^- is a spectator species under the experimental conditions used in this work.[15]

Direct proof for covalent anchoring of the Cu centers was obtained by infrared absorptions observed in the 1000−450

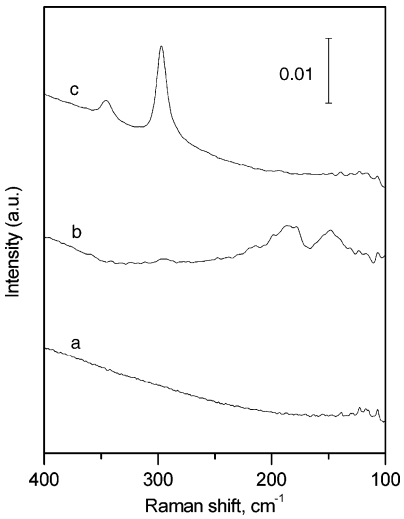

Figure 6. FT-Raman spectra of (a) $TiCu^{I}$−MCM-41 after heating to 250 °C, (b) Cu_2O (2 wt %) mechanically mixed with MCM-41, and (c) CuO (2 wt %) mechanically mixed with MCM-41. Spectra were recorded at 2 cm^{-1} resolution.

cm^{-1} region. Only two intervals of this region are obscured by silicate lattice absorptions (1250−970 cm^{-1}, asymmetric SiO_2 stretch; 820−780 cm^{-1}, symmetric SiO_2 stretch), leaving a window open for the detection of metal−oxygen bond modes. For Cu−MCM-41, two modes associated with the metal center are observed, namely, a shoulder at 930 cm^{-1} and a band at 648 cm^{-1} (Figure 4). The 930 cm^{-1} band is typical for Si−O stretching modes perturbed by the presence of a metal center and is quite insensitive to the nature of the metal.[20] It is red-shifted by 40 cm^{-1} from the Si−O mode of the neat silicate at 970 cm^{-1} (the apparent peak around 960 cm^{-1} of Figure 4 reflects incomplete spectral subtraction of this intense silica absorption for sample and background). The band at 648 cm^{-1} (full width at half-maximum (fwhm) = 20 cm^{-1}) agrees well with the Cu^{I}−O stretch mode of Cu^{I} oxide thin films in the 645−620 cm^{-1} range reported in the literature[23] (the closeness of the Cu−O stretch mode of Cu−O−Si and Cu−O−Cu linkages indicates little coupling between the Cu−O and Si−O modes, consistent with the small shift of the Si−O stretch of Si−O−Cu and Si−O−Si already noted above). Trace b of Figure 4 shows that the two bands are retained upon removal of the residual CH_3CN ligands by heating to 200 °C in a vacuum. We conclude that exposure of the $Cu^{I}(NCCH_3)_4^{+}$ complex to the silicate sieve results in covalent anchoring of the Cu center by at least one Cu^{I}−O−Si linkage, with other valences possibly satisfied by coordination of the Cu^{+} center with surface siloxane (Si−O−Si) oxygens.[24]

For the bimetallic sieve $TiCu^{I}$−MCM-41, the Cu^{I}−O absorption is slightly red-shifted to 642 cm^{-1}, considerably broader (fwhm = 30 cm^{-1}), and twice as intense as that for the monometallic Cu^{I}−MCM-41 material (Figure 5). For the intensity comparison, the bands were normalized for identical silicate wafer thickness by aid of the 1860 cm^{-1} Si−O overtone absorption. Since the DRS of $TiCu^{I}$−MCM-41 does not exhibit a distinct onset around 630 nm characteristic of Cu_2O custers,[25] assignment to Cu−O−Cu moieties can be ruled out. This is further confirmed by the complete absence of Cu_2O absorptions in the FT-Raman spectrum in the 200−100 cm^{-1} region. In Figure 6, the Raman spectrum of $TiCu^{I}$−MCM-41 (trace a) is compared with that of a mechanical mixture of 2% Cu_2O and MCM-41 (trace b), which shows strong Raman bands at 193 and 154 cm^{-1}. Moreover, the 642 cm^{-1} band coincides with

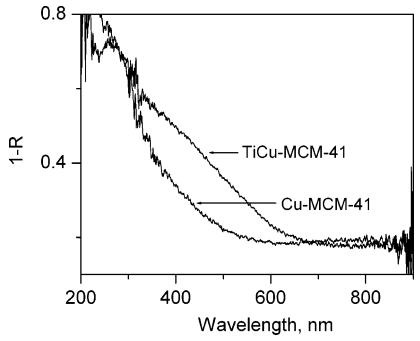

Figure 7. UV−vis diffuse reflectance spectrum of $TiCu^{I}$−MCM-41 and Cu^{I}−MCM-41 wafers after heating in a vacuum at 200 °C for 12 h.

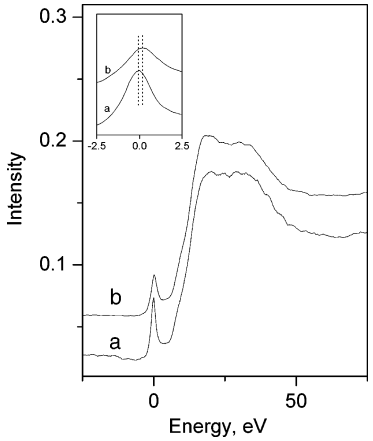

Figure 8. XANES spectra of (a) Ti−MCM-41 and (b) $TiCu^{I}$−MCM-41. Data were recorded at 0.2 eV resolution and a dwell time of 2 s. The insert shows the preedge peaks in an expanded energy scale of clarity. The A_1−T_2 preedge peak (4968 eV) of the Ti−MCM-41 material is taken as the origin of the energy scale.

the Cu^{I}−O infrared absorption observed upon grafting of the $Cu^{I}(NCCH_3)_4^{+}$ complex onto porous TiO_2 using the same procedure as for the anchoring onto the mesoporous silicate. As expected, the material showed the yellow color of the $TiOCu^{I}$ MMCT absorption tail already observed in the case of $TiCu^{I}$−MCM-41.[15] This strongly indicates that ν(Cu−O) of Ti−O−Cu^{I} absorbs at 642 cm^{-1}. Cu^{I}−O−Si linkages may contribute to the absorption as well. Comparison of Figures 4 and 5 shows that the absorption intensity in the 950−900 cm^{-1} region is substantially higher for the $TiCu^{I}$−MCM-41 material than that for the Cu^{I} sieve, which is due to the presence of Si−O modes perturbed by Cu and by Ti[20] in the case of the bimetallic silicate. The spectra of Figure 5 also confirm that the Si−O−Cu (Si−O−Ti) bands and the Cu^{I}−O stretch absorption remain intact after removal of residual CH_3CN ligands by heating. The integrity of the covalent Ti−O−Cu^{I} and Cu^{I}−O−Si linkages upon heating to 200 °C under vacuum is mirrored in the retention of the visible MMCT absorption under this treatment, as shown in Figure 7. No formation of Cu_2O or CuO was detected by FT-Raman (Figure 6).[26] We conclude that the $TiCu^{I}$−MCM-41 sieve consists of anchored binuclear Ti−O−Cu units along with isolated Cu or Ti sites.

While the infrared and optical data do not allow us to estimate the ratio of Cu linked to Ti versus isolated Cu centers, comparison of Ti preedge X-ray absorption spectra of $TiCu^{I}$−MCM-41 and Ti−MCM-41 nevertheless suggests that the fraction of Ti engaged in binuclear moieties is not small. As can be seen from Figure 8, grafting of Cu onto Ti−MCM-41 results in a decrease of the preedge peak intensity and a slight

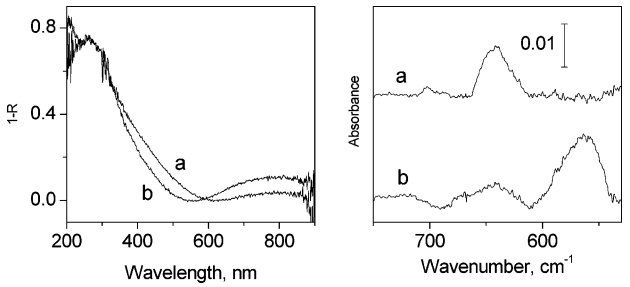

Figure 9. Optical diffuse reflectance and FT-IR spectra upon exposure of $TiCu^{I}$−MCM-41 sieve to air at room temperature: (a) evacuated sample; (b) after exposure to air. For background subtraction, the spectrum of neat MCM-41 was used. The small Cu^{II} band at 800 nm of the evacuated TiCu−MCM-41 sample (curve a) originates from exposure of the material to air during pressing of the wafer.

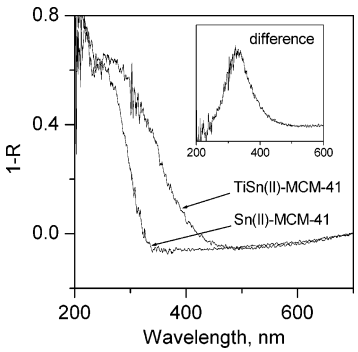

Figure 10. UV−vis DRS spectra of $TiSn^{II}$−MCM-41 and Sn^{II}−MCM-41 after heating under vacuum. The insert shows the difference of $TiSn^{II}$ and Sn^{II} spectra.

shift of 0.2 eV to higher energy. Accuracy and reproducibility of the shift was verified by alternating measurements between the two samples under identical experimental conditions. These energy and intensity changes of the XANES peak are identical to the spectral changes reported upon distortion of the tetrahedral Ti by Ti−OH → Ti−O−O−butyl substitution in Ti−MCM-41.[27] Therefore, the observed effect is consistent with a distortion of the tetrahedral TiOH group by the formation of a Ti−O−Cu linkage. It is unlikely that the changes would be noticeable if only a small fraction of the Ti centers were part of a binuclear moiety.

Exposure of the $TiCu^{I}$−MCM-41 sieve to 1 atm of O_2 gas or air led to a decrease of the 300−600 nm absorption under concurrent growth of a broad band centered at 800 nm (Figure 9). The latter is characteristic for the d−d absorption of Cu^{II}.[21,28] The decrease of the MMCT absorption is not fully apparent in this spectrum because of overlap with the increasing Cu^{II}−O LMCT band in the near-UV region.[21,29] As expected, FT-IR monitoring of the oxidation revealed a loss of $\nu(Cu^{I}-O)$ at 642 cm^{-1} and growth of a band at 560 cm^{-1} (Figure 9). The new absorption is in agreement with $\nu(Cu^{II}-O)$ modes reported for Cu^{II} complexes,[30] CuO thin films,[23b,c] or basic Cu^{II} salts.[31] These observations strongly support the assignment of the 300−600 nm absorption to the MMCT chromophore. Cu^{II} centers anchored on MCM-41 pore surfaces have been reported to have Cu−O−Si linkages that are displaced by coordination to adsorbed H_2O.[32] Experiments are in progress to investigate the stability of the moiety upon exposure to various adsorbents, including the fate of the Cu coordination upon oxidation.

B. $TiSn^{II}$−MCM-41. Grafting of Sn^{II} onto Ti−MCM-41 using $SnCl_2 \cdot 2H_2O$ dissolved in acetonitrile as a precursor gave a material whose optical spectrum is shown in Figure 10. The bimetallic sieve has an intense absorption extending to 470 nm

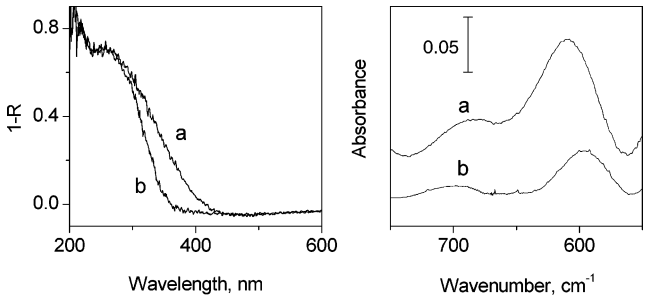

Figure 11. Optical DRS (left) and FT-IR (right) spectra of $TiSn^{II}$−MCM-41 upon exposure to air at room temperature: (a) evacuated sieve; (b) after exposure to air. For background subtraction of the FT-IR traces, the spectrum of neat MCM-41 was used.

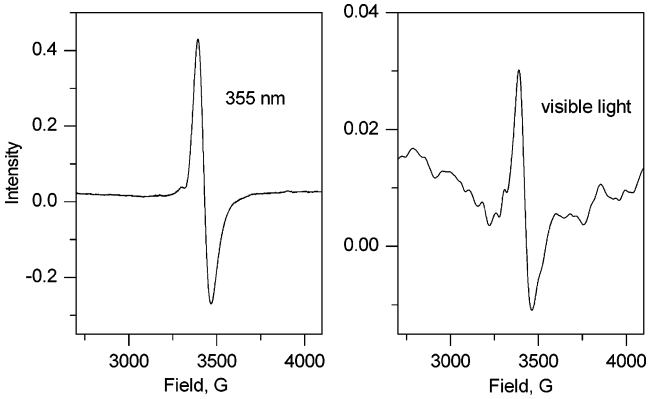

Figure 12. EPR spectra of $TiSn^{II}$−MCM-41 irradiated with 355 nm light (left) and visible (> 400 nm) light (right) at 77 K for 30 min. EPR spectra were collected at 20 K.

that is absent in monometallic Sn^{II}−MCM-41. The only assignment we can conceive of is $Ti^{IV}/Sn^{II} \rightarrow Ti^{III}/Sn^{III}$ MMCT, and the corresponding absorption profile is given in the insert of Figure 10. The shorter wavelength onset of the charge-transfer transition compared to the $TiCu^{I}$ site reflects the instability (high reduction potential) of Sn^{III}.

FT-IR spectroscopy revealed that all CH_3CN ligands are removed by evacuation at room temperature. Exposure of the $TiSn^{II}$−MCM-41 sieve to air resulted in a decrease of the MMCT absorption and a shift of a band at 610 cm^{-1} to 595 cm^{-1}. These effects are shown in Figure 11. The 610 cm^{-1} absorption (fwhm = 44 cm^{-1}) and the visible chromophore were also observed when grafting Sn^{II} onto porous TiO_2, indicating that it is mainly due to Sn^{II}−O−Ti linkages (Sn−O−Sn groups are ruled out because of the absence of black SnO clusters).[15] Frequency of the Sn^{II}−O mode and modest red shift upon oxidation to Sn^{IV} agree with literature data on complexes and thin Sn oxide films.[33] We conclude that the UV−vis MMCT chromophore originates from a covalently anchored Ti^{IV}−O−Sn^{II} moiety.

Irradiation of the MMCT chromophore of the evacuated $TiSn^{II}$−MCM-41 powder with 355 nm light of a Nd:YAG laser at 160 mW cm^{-2} for 30 min led to the $g = -1.907$ EPR signal shown in Figure 12, assigned to Ti^{3+}. A yield of 9% was calculated using Cu^{II} acetate as a standard. The same signal was also observed upon shining visible light of a filtered W-source for 30 min at 77 K (Corning filter #3-75, λ > 400 nm, 2 W). No EPR signal was detected upon visible-light irradiation of a MCM-41 sieve that contained only grafted Sn^{II} or Ti. Thermally induced reduction of Ti by Sn^{II} is ruled out because the sample was pretreated at 200 °C under evacuation, and no Ti^{3+} signal was detected. We conclude that excitation of the Ti^{IV}−O−Sn^{II} moiety leads to activation of Ti under

visible light. Assignment was confirmed by observation of an identical EPR signal following excitation of Ti−MCM-41 with 266 nm light at 77 K, which is known to generate Ti^{3+} via excitation of the Ti−O LMCT transition.[15,34] In the latter case, the longevity of the charge separation is most likely due to hopping of the O hole across the silica framework and trapping in a defect site. In the case of TiSn−MCM-41, we attribute the buildup of Ti^{3+} at cryogenic temperature to trapping of the electron by Ti centers as the unstable Sn^{III},[35] generated by MMCT excitation, spontaneously converts to Sn^{IV}.

C. Relationship to Other Bimetallic Silicate Sieves. The grafted $Ti^{IV}-O-Cu^{I}$ and $Ti^{IV}-O-Sn^{II}$ MMCT moieties observed here are the localized, two-center chromophores that underlie the visible absorption phenomena of more complex bimetallic materials reported recently by several laboratories. In these composites, a single metal center is linked to an oxide cluster of a second metal, such as O−Ti−O−Ti−O chains in the case of Nb-, Cr-, Fe-, or Co-substituted microporous ETS-10.[36] Furthermore, colored materials have been reported for MCM-41 silicates containing V, Cr, or Fe centers in the framework and TiO_2 particles in the channels.[37] In this context, metal-to-particle charge-transfer at TiO_2 particles for electron injection into the conduction band should be mentioned.[38] Also, ion implantation of V, Cr, Mn, Fe, Ni, and other transition metals into TiO_2 particles or framework metal-containing silicates and aluminosilicates has been used to generate visible absorption properties.[39] The stepwise assembly of single metal centers on pore surfaces shown here allows spectroscopic characterization of the underlying binuclear unit and opens up the exploration of the MMCT-induced chemistry of well-defined redox sites with a completely inorganic ligand environment in mesoporous silicate sieves.

4. Conclusions

In summary, assembly of organic-free bimetallic $Ti-O-Cu^{I}$ and $Ti-O-Sn^{II}$ MMCT moieties on mesoporous silicate surfaces with each metal in a preselected oxidation state has been demonstrated. The method is based on the use of precursors with labile CH_3CN ligands that are readily substituted by surface TiOH or SiOH groups. Difference optical DRS and FT-IR spectroscopy allowed us to identify the $Cu^{I}-O$ ($Sn^{II}-O$) bond modes associated with the visible $Ti^{IV}-O-Cu^{I}$ and $Ti^{IV}-O-Sn^{II}$ MMCT chromophores. In the case of $TiSn^{II}$−MCM-41, electron transfer upon visible-light excitation of the MMCT transition was demonstrated by recording of the EPR signal of Ti^{3+} at cryogenic temperature. Activation of Ti centers by MMCT excitation of heterodinuclear moieties anchored on mesoporous silica surfaces offers opportunities for exploring demanding photochemical transformations previously limited to UV light.

Acknowledgment. This work was supported by the Director, Office of Science, Office of Basic Energy Sciences, Division of Chemical, Geological and Biosciences of the U. S. Department of Energy under contract No. DE-AC03-76SF00098. The authors thank Dr. Vittal Yachandra and Dr. Junko Yano for assistance with the EPR measurements.

Supporting Information Available: FT-IR spectra displaying precursor ligand, counterion, and solvent absorption regions upon evacuation of $TiCu^{I}$−MCM-41 and $TiSn^{II}$−MCM-41 materials. UV−vis DRS of porous TiO_2 surfaces upon grafting of Cu^{I} and Sn^{II} precursors and exposure to air. EPR spectra of Ti−MCM-41 recorded after excitation at 266 or 355 nm at cryogenic temperature. This material is available free of charge via the Internet at http://pubs.acs.org.

References and Notes

(1) (a) Anpo, M.; Zhang, S. G.; Yamashita, H. *Stud. Surf. Sci. Catal*. **1996**, *101*, 941. (b) Zhang, S. G.; Ichihashi, Y.; Yamashita, H.; Tatsumi, T.; Anpo, M. *Chem. Lett.* **1996**, 895. (c) Zhang, S. G.; Fujii, Y.; Yamashita, H.; Koyano, K.; Tatsumi, T.; Anpo, M. *Chem. Lett*. **1997**, 659. (d) Anpo, M.; Yamashita, H.; Ikeue, K.; Fujii, Y.; Zhang, S. G.; Ichihashi, Y.; Park, D. R.; Suzuki. Y.; Koyano, K.; Tatsumi, T. *Catal. Today* **1998**, *44*, 327. (e) Matsuoka, M.; Anpo, M. *J. Photochem. Photobiol. C: Photochem. Rev.* **2003**, *3*, 225.

(2) (a) Ulagappan, N.; Frei, H. *J. Phys. Chem. A* **2000**, *104*, 490. (b) Yeom, Y. H.; Frei, H. *J. Phys. Chem. A* **2002**, *106*, 3350. (c) Ulagappan, N.; Frei, H. *J. Phys. Chem. A* **2000**, *104*, 7834. (d) Yeom, Y. H.; Frei, H. *J. Phys. Chem. A* **2001**, *105*, 5534. (e) Lin, W.; Frei, H. *J. Am. Chem. Soc*. **2002**, *124*, 9292.

(3) Howe, R. F.; Krisnandi, Y. K. *Chem. Commun.* **2001**, 1588.

(4) Llabres i Xamena, F.; Calza, P.; Lamberti, C.; Prestipino, C.; Darwin, A.; Bordiga, S.; Pelizzetti, E.; Zecchina, A. *J. Am. Chem. Soc.* **2003**, *125*, 2264.

(5) Blasse, G. *Struct. Bonding* **1991**, *76*, 153.

(6) (a) Oldroyd, R. D.; Thomas, J. M.; Sankar, G. *Chem. Commun.* **1997**, 2025. (b) Oldroyd, R. D.; Sankar, G.; Thomas, J. M.; Ozkaya, D. *J. Phys. Chem. B* **1998**, *102*, 1849.

(7) (a) Luan, Z.; Kevan, L. *J. Phys. Chem. B* **1997**, *101*, 2020. (b) Luan, Z.; Meloni; P. A.; Czernuszewicz, R. S.; Kevan, L. *J. Phys. Chem. B* **1997**, *101*, 9046.

(8) (a) Maschmeyer, T.; Rey, F.; Sankar, G.; Thomas, J. M. *Nature* **1995**, *378*, 159. (b) Morey, M. S.; Stucky, G. D.; Schwarz, S.; Froba, M. *J. Phys. Chem. B* **1999**, *103*, 2037. (c) DeVos, D. E.; Dams, M.; Sels, B. F.; Jacobs, P. A. *Chem. Rev.* **2002**, *102*, 3615 and references therein.

(9) Lin, W.; Cai, Q.; Pang, W.; Yue, Y.; Zou, B. *Microporous Mesoporous Mater*. **1999**, *33*, 187.

(10) Yeom, Y. H.; Frei, H. *J. Phys. Chem. A* **2001**, *105*, 5334.

(11) Babonneau, F.; Doeuff, S.; Leaustic, A.; Sanchez, C.; Cartier, C.; Verdaguer, M. *Inorg. Chem.* **1988**, *27*, 3166.

(12) Sankar, G.; Thomas, J. M. *Top. Catal*. **1999**, *8*, 1.

(13) Blatter, F.; Moreau, F.; Frei, H. *J. Phys. Chem*. **1994**, *98*, 13403.

(14) Marchese, L.; Gianotti, E.; Dellarocca, V.; Maschmeyer, T.; Rey, F.; Coluccia, S.; Thomas, J. M. *Phys. Chem. Chem. Phys*. **1999**, *1*, 585.

(15) Spectra shown in Supporting Information.

(16) Beck, J. S.; Vartuli, J. C.; Roth, W. J.; Leonowicz, M. E.: Kresge, C. T.; Schmitt, K. D.; Chu, C. T. W.; Olsen, D. H.; Sheppard, E. W.; McCullen, S. B.; Higgins, J. B.; Schlenker, J. L. *J. Am. Chem. Soc.* **1992**, *114*, 10834.

(17) Blatter, F.; Frei, H. *J. Am. Chem. Soc*. **1994**, *116*, 1812

(18) Buschmann, W. E.; Miller, J. S. *Chem.—Eur. J.* **1998**, *4*, 1731.

(19) *Handbook of Chemistry and Physics*; West, R. C., Ed.; CRC Press: Cleveland, 1975; p F-216.

(20) (a) Morey, M. S.; O'Brien, S.; Schwarz, S.; Stucky, G. D. *Chem. Mater*. **2000**, *12*, 898. (b) Morey, M. S.; Bryan, J. D.; Schwarz, S.; Stucky, G. D. *Chem. Mater.* **2000**, *12*, 3435. (c) Van Der Voort, P.; Morey, M.; Stucky, G. D.; Mathieu, M.; Vansant, E. F. *J. Phys. Chem. B* **1998**, *102*, 585. (d) Marchese, L.; Gianotti, E.; Dellarocca, V.; Maschmeyer, T.; Rey, F.; Coluccia, S.; Thomas, J. M. *Phys. Chem. Chem. Phys*. **1999**, *1*, 585. (e) Raimondi, M. E.; Gianotti, E.; Marchese, L.; Martra, G.; Maschmeyer, T.; Seddon, J. M.; Coluccia, S. *J. Phys. Chem. B* **2000**, *104*, 7102. (f) Bouh, A. O.; Rice, G. L.; Scott, S. L. *J. Am. Chem. Soc.* **1999**, *121*, 7201.

(21) Texter, J.; Strome, D. H.; Herman, R. G.; Klier, K. *J. Phys. Chem.* **1977**, *81*, 333.

(22) Ferraro, J. R.; Walker, W. R. *Inorg. Chem.* **1965**, *4*, 1382.

(23) (a) Persson, D.; Leygraf, C. *J. Electrochem. Soc.* **1993**, *140*, 1256. (b) Ogale, S. B.; Bilurkar, P. G.; Mate, N.; Kanetkar, S. M.; Parikh, N.; Patnaik, B. *J. Appl. Phys.* **1992**, *72*, 3765. (c) Padiyath, R.; Seth, J.; Babu, S. V. *Thin Solid Films* **1994**, *239*, 8.

(24) (a) Nozaki, C.; Lugmair, C. G.; Bell, A. T.; Tilley, T. D *J. Am. Chem. Soc.* **2002**, *124*, 13194. (b) Fujdala, K. L.; Drake, I. J.; Bell, A. T.; Tilley, T. D. *J Am. Chem. Soc.* **2004**, *126*, 10864.

(25) Bordiga, S.; Paze, C.; Berlier, G.; Scarano, D.; Spoto, G.; Zecchina, A.; Lamberti, C. *Catal. Today* **2001**, *70*, 91.

(26) Xu, J. F.; Ji, W.; Shen, Z. X.; Li, W. S.; Tang, S. H.; Ye, X. R.; Jia, D. Z.; Xin, X. Q. *J. Raman Spectrosc.* **1999**, *30*, 413.

(27) Sankar, G.; Thomas, J. M.; Catlow, C. R. A.; Barker, C. M.; Gleeson, D.; Kaltsoyannis, N. *J. Phys. Chem. B* **2001**, *105*, 9028.

(28) Lever, A. B. P. *Inorganic Electronic Spectroscopy*, 2nd ed.; Elsevier: Amsterdam, 1984; p 355.

(29) Zhu, Z. H.; Zhu, H. Y.; Wang, S. B.; Lu, G. Q. *Catal. Lett.* **2003**, *91*, 73.

(30) McWhinnie, W. R. *J. Inorg. Nucl. Chem.* **1965**, *27*, 1063.

(31) Frost, R. L.; Martens, W. N.; Rintoul, L.; Mahmutagic, E.; Kloprogge, J. T. *J. Raman Spectrosc*. **2002**, *33*, 252.

(32) (a) Gao, Y.; Konovalova, T. A.; Lawrence, J. N.; Smitha, M. A.; Nunley, J.; Schad, R.; Kispert, L. D. *J. Phys. Chem. B* **2003**, *107*, 2459. (b) Poppl, A.; Newhouse, M.; Kevan, L. *J. Phys. Chem.* **1995**, *99*, 10019.

(33) Adams, D. M. *Metal−Ligand and Related Vibrations*; Edward Arnold Publishers: London, 1967; p 235.

(34) Ghorbel, A.; Tuel, A.; Jorda, E.; Ben Taarit, Y.; Naccache, C. *Stud. Surf. Sci. Catal.* **1995**, *97*, 471.

(35) Booth, R. J.; Starkie, H. C.; Symons, M. C. R. *J. Chem. Soc., Dalton Trans.* **1973**, 2233.

(36) (a) Eldewik, A.; Luca, V.; Singh, N. K.; Howe, R. F. *Proc. 12th Int. Zeol. Conf.*; Treacy, M. M. J.; Marcus, B. K.; Bisher, M. E.; Higgins, J. B., Eds.; Materials Research Society: Warrendale, PA, 1999; p 1507. (b) Rocha, J.; Brandao, P.; Pedro de Jesus, J.; Phillippou, A.; Anderson, M. W. *Chem. Commun.* **1999**, 471. (c) Brandao, P.; Phillippou, A.; Anderson, M. W. *Phys. Chem. Chem. Phys.* **2001**, *3*, 1773. (d) Eldewik, A.; Howe, R. F. *Microporous Mesoporous Mater.* **2001**, *48*, 65.

(37) (a) Reddy, E. P.; Davydov, L.; Smirniotis, P. G. *J. Phys. Chem. B* **2002**, *106*, 3394. (b) Davydov, L.; Reddy, E. P.; France, P.; Smirniotis, P. G. *J. Catal.* **2001**, *203*, 157.

(38) (a) Khoudiakov, M.; Parise, A. R.; Brunschwig, B. S. *J. Am. Chem. Soc.* **2003**, *125*, 4637. (b) Kelly, C. A.; Meyer, G. J. *Coord. Chem. Rev.* **2001**, 211, 295.

(39) (a) Anpo, M. *Stud. Surf. Sci. Catal.* **2000**, *130*, 157. (b) Takeuchi, M.; Yamashita, H.; Matsuoka, M.; Anpo, M.; Hirao, T.; Itoh, N.; Iwamoto, N. *Catal. Lett.* **2000**, *67*, 135. (c) Anpo, M.; Takeuchi, M.; Ikeue, K.; Dohshi, S. *Curr. Opin. Solid Mater. Sci.* **2002**, *6*, 381. (d) Yamashita, H.; Harada, M.; Misaka, J.; Takeuchi, M.; Neppolian, B.; Anpo, M. *Catal. Today* **2003**, *84*, 191.